IEEE Access
Multidisciplinary | Rapid Review | Open Access Journal

Received July 15, 2019, accepted July 31, 2019, date of publication August 19, 2019, date of current version August 29, 2019.

Digital Object Identifier 10.1109/ACCESS.2019.2936250

Wireless Power Transfer Based on Microwaves and Time Reversal for Indoor Environments

BING LI[1,2,3], SHIQI LIU[4,5], HONG-LIN ZHANG[6], BIN-JIE HU[6], (Senior Member, IEEE), DESHUANG ZHAO[2], (Member, IEEE), AND YINGKUN HUANG[1]

[1]School of Electrical Engineering, Southwest Jiaotong University, Chengdu 610031, China
[2]School of Physics, University of Electronic Science and Technology of China, Chengdu 610054, China
[3]Institut Langevin, 75005 Paris, France
[4]College of Information Engineering, Shenzhen University, Shenzhen 518060, China
[5]Southwest China Research Institute of Electronic Equipment, Chengdu 610036, China
[6]School of Electronic and Information Engineering, South China University of Technology, Guangzhou 510641, China

Corresponding authors: Bing Li (bllijess@outlook.com), Shiqi Liu (liu.shiqi@outlook.com), and Hong-Lin Zhang (eezhl@scut.edu.cn)

This work was supported in part by the Fundamental Research Funds for the Central Universities under Grant 2682017CX046, in part by the National Natural Science Foundation of China under Grant 61671133 and Grant 61871193, in part by the Sichuan Applied Basic Research Project under Grant 19YYJC0025, in part by the Key Project of Guangdong Natural Science Foundation under Grant 2018B030311049, and in part by the Fellowship from Chinese Scholarship Council (CSC).

ABSTRACT Resorting to power accurate delivery for wireless power transfer (WPT) based on microwaves, a theory and method based on time reversal (TR) for WPT in 3D indoor environments are presented in this paper. Conventional WPT methods have the limitations of requiring that the elements on power source array (PSA) must have the same structure and regular arrangement. Unlike those conventional methods, the PSA used in this paper can be constructed by any omnidirectional antenna elements with any structure and any arrangement, whose principles are based on the auto-match of antenna radiation and environment adaptability of TR. Moreover, compared with those conventional methods, which perform complex multi-objective optimizations of beam pattern cost-functions at each frequency for getting excitation of PSA, the proposed algorithm can obtain PSA's excitation over a wide frequency range only by a single run of TR and Fourier transform operations. In addition, by weighting the time reversed charging request signal from powered devices, the interference caused by different observing elevation angles and amplitude difference among each channel can be suppressed effectively. At last, multi-powered devices placed arbitrarily can be charged simultaneously, and get similar power from PSA without power unfairness by our proposed algorithm.

INDEX TERMS
3D indoor environment, auto-match of antenna radiation and channel, microwave, time reversal, wireless power transfer.

I. INTRODUCTION

Wireless power transfer (WPT) working in the microwave range gathers a considerable interest for many potential applications [1]–[5], especially the scenarios where the electrical wired devices is unfeasible or cost ineffective, such as solar satellites [6], [7], space stations [8], unmanned aerial vehicle [9], and corrosive environment.

According to the distance of power transfer, operating principle, frequency band and the scenarios of application, three kinds of WPT are researched these days, namely, short-range, midrange and long-range WPT. Therein, short-range WPT works by means of near-field coupling, which guarantees the transmission efficiency up to 90% in some ways, and is widely used in radio-frequency identification (RFID) [10], biomedical implanted devices [11] and the most wireless charging of consumer electronics. However, it can be only operated over distances of the order of wavelength, and has a great decline of efficiency when the air gap between power sources and devices increases or any misalignment occurs. Midrange WPT is usually achieved by magnetic resonance [12], by which electronic devices can be powered at distances longer than 10 m [13]. But, the power source equipments, which are usually coils, are

The associate editor coordinating the review of this article and approving it for publication was Yingsong Li.

big compared with powered devices [14], [15]. In addition, this technique requires the powered devices have the same resonance frequency as that of power source [16]. Although this requirement can suppress the waste of energy impinging on non-powered devices, the application is still limited. Additionally, the efficiency of WPT based on magnetic resonance drops quickly when the air gap between power sources and devices changes [16]. Moreover, these two WPT methods discussed above are also called non-radiative WPT, which is different from the long-range WPT using microwave radiation theory to transfer energy wirelessly. Specifically, long-range WPT is exploited from the view of electromagnetic far-field radiation, requires the transmission of microwave from the generating point to one or more faraway receiver, and power wireless electronic devices over moderate to long distances, whose excitation can cover a wide range. Namely, this kind of WPT does not require the powered devices have the same resonance frequency like the condition of using magnetic resonance. Although the efficiency is still decline with the increasement of distance and misalignment between power souces and devices, the technology of power accurate delivery can alleviate this problem [17].

Besides, although the concept and fundamental of WPT based on microwave is not completely new, since they are loosely related to those of radar and wireless communications' theories [18], [19], the long-term viability of electronic devices needs to address power accurate delivery through a perspective combined with specific tools and approaches.

Nowadays, the most popular solutions to address the above problems are using beamforming algorithms or retro-reflective methodologies in WPT [20]–[24]. The general principle of these two methods is generating pencil beams to focus the power in a narrow direction towards the powered devices. By carefully shaping the transmitted waveform at each antenna over the whole operation frequency band, beamforming is able to control the collective behavior of the radiation pattern of power source array (PSA). Generally, the larger number of antennas on PSA, the shaper power beam is able to be generated towards the powered device's spatial direction [25].

However, these two methods can steer a signal sharp beam to maximize the harvested power towards only one powered device. When there are more than one electronic devices needed to be charged, this method may result in severe power unfairness among these powered devices. In this case, the PSA needs to generate multiple optimized function to produce multi-power beams in different directions of the corresponding powered devices to balance the unfairness. This operation is not only complex because single beam function should be optimized for each powered device, but also has a limitation that the antennas on PSA must have the same sturcture and regular arrangement. Thus, these two methods lack the environment and structure adaptability, and are not suitable for unfixed devices since the optimal function need to be reconstructed when the positions of powered devices are changed. Additionally, the retro-reflective methodology [24] just can obtain the optimal beam at one single frequency by a single run of optimization function, which is time consuming for wideband systems.

Therefore, it can be seen clearly that how to build optimal function adaptively according to the different spatial channels and multi-powered devices' positions is the key to break the bottleneck of conventional WPT algorithms and further develop WPT based on microwaves.

Time reversal (TR) is a good candidate to achieve this object, because its superiorities of adaptive spatio-temporal focusing and broadband on communications [26], [27], radar imaging [28], location [29] and shaping spatial fields [30]. The focusing property of TR was firstly executed by Fink [31] in acoustic field, and reported subsequently in microwaves by Lerosey [32]. These researches disclose that TR has the ability of controlling wave in complicated media, which contains multipath and multi-reflections. Specifically, TR can take advantage of multipath to focus the wave on the wanted direction further, espcially in complex media [29]. Therein, multipath is generally recognized as noise or clutter and mitigated/ignored in conventional communication, imaging algorithms etc. Thus, TR has a great potential to adaptively focus power on multi-position, where the powered devices are placed, and adaptively direct power towards multi-powered devices over the whole wide operating frequency band of PSA. Even so, its application in WPT has been studied just recent several years [17], [33]. And the researches are just limited in 2D environment and charging single electronic device. Its applications on charging multi-powered devices simultaneously is seldom researched. Further, the problem of power unfairness impinging on multi-powered devices is unsolved, especially in 3D environment.

Based on this, this paper proposes a power accurate delivery method based on TR, which is suitable for 3D indoor WPT environments and yields many advantages such as:

(1) Improvement of efficiency of WPT (evaluated by power collection efficiency (PCE) in this paper): spatio-temporal focusing property of TR increases the signal to interference and noise ratio impinging on the powered devices.

(2) Suppression of interference to non-powered devices (evaluated by sidelobe in this paper): by taking advantages of multipath rather than ignoring or mitigating it, TR achieves more accurate power delivery with small sidelobes.

(3) Increased coverage applications: a wideband excitation of PSA can be achieved by a single run of TR operation and Fourier transformation. And, the channel matched delivering power can also be obtained for the whole wide frequency band at a time. Besides, those frequencies can cover working bands of multi-kind/multi electronic devices, which allows an increased coverage applications.

Furthermore, in this paper, a weighted method is developed to address the power unfairness problem. This method can suppress the interference from different observing elevation angles and amplitude difference among each channel.

The remainder of this paper is organised as follows. Section II provides the algorithm and method used throughout

this paper. The corresponding numerical experiments and analyses are discussed in Section III. Finally, Section IV concludes this paper. Additionally, the electronic devices needed to be charged are called powered devices throughout this paper, and send charging request signal when they are in low battery states.

II. METHODS

In this study, we aim to charge any device wirelessly in 3D indoor environments, such as living room, office, warehouse and parking lot etc. The PSA can be fixed at anywhere in the room, for example, on the side walls or the ceiling. Here, we place PSA on the ceiling for example as shown in Fig.1. The PSA consists of N omnidirectional antennas with any structure and arrangement. Any number of powered devices such as digital camera, laptop, cell phone and electric toothbrush can be positioned at anywhere in the room as well. Here, the total number of powered devices is M. Assume that the distance between PSA plane and power receiving plane (PRP) is L. The powered devices are placed arbitrarily in the PRP. We choose the center of ceiling as the origin of coordinate. Define θ as elevation angle and ϕ as azimuth angle.

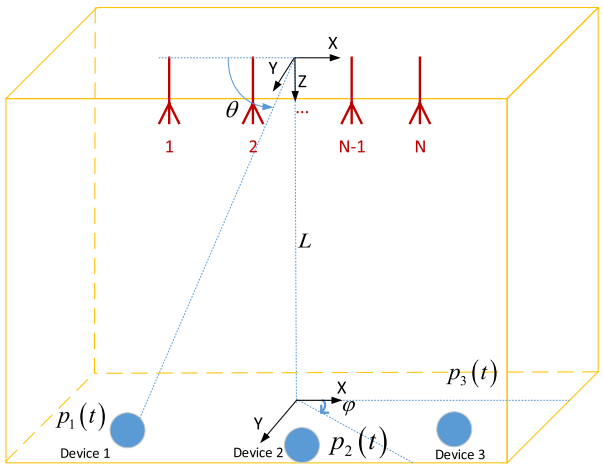

FIGURE 1. Illustration of WPT in a 3D indoor environment.

First, we consider about the case of only one powered device. Take the radiation pattern of PSA into account, when only the m^{th} powered device placed at (θ_m, φ_m) sends charging request signal $p_m(t), m = 1, 2, \cdots, M$, the received signal at PSA can be expressed as

$$y(t) = \sum_{n=1}^{N} p_m(t) \otimes h_{mn}(t) \otimes f_n(\theta_m, \varphi_m, t) \tag{1}$$

where "$\otimes$" denotes convolution operator, $f_n(\theta_m, \varphi_m, t)$ is the radiation pattern of the n^{th} antenna of PSA, whose position is (θ_m, φ_m); $h_{mn}(t)$ presents the channel information between the m^{th} powered device and the n^{th} antenna. Its expression can be wrote as

$$h(t) = X \sum_{k=1}^{K} \sum_{q=1}^{Q(k)} a_{qk} \delta(t - T_k - \tau_{qk}) \tag{2}$$

which is chosen according to multipath channel model in IEEE802.15.3a [34], [35]. Therein, X is log normal random variable representing the gain of channel amplitude. K is the total number of cluster, which indicates the form of charging request signal arriving at PSA through multipath. $Q(k)$ is the total number of the k^{th} cluster's path. a_{qk} is the coefficient of the q^{th} path in the k^{th} cluster. T_k is the arrival time of the k^{th} cluster. τ_{qk} is the delay of the q^{th} path in the k^{th} cluster.

We take TR operation on the received charging request signal at PSA, and get the corresponding expression as

$$y_{TR}(t) = \sum_{n=1}^{N} p_m(-t) \otimes h_{mn}(-t) \otimes f_n(\theta_m, \varphi_m, -t) \tag{3}$$

And corresponding expression in frequency domain can be obtained by Fourier transformation as

$$Y_{TR}(\omega) = \sum_{n=1}^{N} P_m^*(\omega) H_{mn}^*(\omega) F_n^*(\theta_m, \varphi_m, \omega) \tag{4}$$

where superscript "$*$" denotes conjugation operator. Each antenna takes its respective time reversed frequency signal as excitation. It can be seen obviously that this synthesized excitation is wideband and can be achieved by a single run of TR and Fourier transform operations.

Next, we will prove our proposed power accurate delivery method are suitable for the whole frequency band without optimizing at each frequency. Because of the reciprocity of antenna radiation, the received mode of antenna is the same as the transmitted mode. Thus, we can get the radiation signal from the n^{th} antenna at all elevation and azimuth angles as

$$S_n(\theta, \varphi, \omega) = P_m^*(\omega) H_{mn}^*(\omega) F_n^*(\theta_m, \varphi_m, \omega) F_n(\theta, \varphi, \omega) \tag{5}$$

Then, the signal received by the original powered device placed at (θ_m, φ_m), which sends charging request signal, can be expressed as

$$\begin{aligned} Y_r(\theta_m, \varphi_m, \omega) &= \sum_{n=1}^{N} S_n(\theta_m, \varphi_m, \omega) H_{mn}(\omega) \\ &= \sum_{n=1}^{N} P_m^*(\omega) H_{mn}^*(\omega) \\ &\quad \times F_n^*(\theta_m, \varphi_m, \omega) F_n(\theta_m, \varphi_m, \omega) H_{mn}(\omega) \\ &= \sum_{n=1}^{N} P_m^*(\omega) |H_{mn}(\omega)|^2 |F_n(\theta_m, \varphi_m, \omega)|^2 \end{aligned} \tag{6}$$

It can be seen clearly that the signal arriving at the original powered device is a focused signal through the same multipath. This does not happen at the positions of non-powered devices. The reason can be explained as follows. The expression of signal impinging on the electronic devices placed at

$\theta_x \subseteq [0, \frac{\pi}{2}]$, $\varphi_x \subseteq [0, 2\pi)$, therein ($\theta_x \neq \theta_m$ or $\varphi_x \neq \varphi_m$), can be obtained as

$$\begin{aligned} Y_r(\theta_x, \varphi_x, \omega) &= \sum_{n=1}^{N} S_n(\theta_x, \varphi_x, \omega) H_{xn}(\omega) \\ &= \sum_{n=1}^{N} P_m^*(\omega) H_{mn}^*(\omega) F_n^*(\theta_m, \varphi_m, \omega) \\ &\quad \times F_n(\theta_x, \varphi_x, \omega) H_{xn}(\omega) \end{aligned} \tag{7}$$

Compared eq.(6) with eq.(7), we can find that the radiation type of each antenna matches towards the powered device adaptively. Namely, $|F_n(\theta_m, \varphi_m, \omega)|^2 > F_n^*(\theta_m, \varphi_m, \omega) F_n(\theta_x, \varphi_x, \omega)$, which is suitable for omnidirectional antennas with any structure and arrangement.

Furthermore, assume all electronic devices are placed in the same plane. When elevation angle is constant, power transmission efficiency is unchanged with the changed azimuth angle, since the distance between devices and PSA is unchanged and the same. However, when the elevation angle is changed, the situation is different. Specifically, when $\theta_x < \theta_m$, the attenuation of $H_{mn}(\omega)$ is smaller than that of $H_{xn}(\omega)$. Thus, $|H_{mn}(\omega)|^2 > H_{mn}^*(\omega) H_{xn}(\omega)$ is always true. Namely, the energy obtained by powered device is always larger than that arriving at other places. When $\theta_x = \theta_m$, the attenuations of $H_{mn}(\omega)$ and $H_{xn}(\omega)$ are almost the same. Thus, $|H_{mn}(\omega)|^2 > H_{mn}^*(\omega) H_{xn}(\omega)$ is also always true, and the energy obtained by powered device is always larger than that arriving at other places as well. When $\theta_x > \theta_m$, the attenuation of $H_{mn}(\omega)$ is larger than that of $H_{xn}(\omega)$. Thus, it is very hard to assess the values of $|H_{mn}(\omega)|^2$ and $H_{mn}^*(\omega) H_{xn}(\omega)$. However, $|H_{mn}(\omega)|^2 > H_{mn}^*(\omega) H_{xn}(\omega)$ can be still hold water when N is large enough. Hence, in this situation, the object that energy obtained by powered device is larger than that impinging on other places can be also achieved with enough antennas.

Nevertheless, the interference occurs when there are multi-powered devices. These devices can not be charged simultaneously by above method even with enough antennas. For addressing this problem, we propose a solution.

Assume all powered devices send the same kind of charging request signal. Namely $P_1(\omega) = P_2(\omega) = \cdots = P_M(\omega)$. At PSA, in order to obtain its own wideband excitation of each antenna, we take TR operation and one-time Fourier transformation on the received charging request signals, which is from M powered devices and propagates through the whole environment. Therein, the expression of the n^{th} antenna's wideband excitation is

$$Y_{TR_n}(\omega) = \sum_{m=1}^{M} P_m^*(\omega) H_{mn}^*(\omega) F_n^*(\theta_m, \varphi_m, \omega) \tag{8}$$

Similarly, the radiation signal at all elevation and azimuth angles of the n^{th} antenna can be illustrated as

$$S_n(\theta, \varphi, \omega) = \sum_{m=1}^{M} P_m^*(\omega) H_{mn}^*(\omega) F_n^*(\theta_m, \varphi_m, \omega) F_n(\theta, \varphi, \omega) \tag{9}$$

Then, we can get the received signal's expression at the i^{th} powered device located at (θ_i, φ_i) as

$$\begin{aligned} &Y_r(\theta_i, \varphi_i, \omega) \\ &= \sum_{m=1}^{M} \sum_{n=1}^{N} P_m^*(\omega) H_{mn}^*(\omega) F_n^*(\theta_m, \varphi_m, \omega) F_n(\theta_i, \varphi_i, \omega) H_{in}(\omega) \\ &= \underbrace{\sum_{n=1}^{N} P_i^*(\omega) |H_{in}(\omega)|^2 |F_n(\theta_i, \varphi_i, \omega)|^2}_{\text{useful signal}} \\ &\quad + \underbrace{\sum_{\substack{m=1 \\ m \neq i}}^{M} \sum_{n=1}^{N} P_m^*(\omega) H_{mn}^*(\omega) F_n^*(\theta_m, \varphi_m, \omega) F_n(\theta_i, \varphi_i, \omega) H_{in}(\omega)}_{\text{interference}} \end{aligned} \tag{10}$$

where $(i = 1, 2, \cdots, M)$. It is obvious that the useful signal is a focused signal, which is focused on the i^{th} (original) powered device. Oppositely, the interference item is not a focused signal, and constructed by the $M-1$ charging request signals from all powered devices except the i^{th} one. Moreover, the function of focused signal is directing energy towards the powered device, while the interference item has negative influence, that may change the direction of focused energy or even worse, such as lead to the direction of focused energy uncontrollable.

Different from the single powered device case, in this case, it is very hard to compare the values of useful signal item and interference item with different elevation angles, since the interference is large. But, with enough antennas, the negative influence of interference item can be alleviated. Specifically, with enough antennas, for the condition of $\theta_i \geq \theta_m$, the attenuation of $H_{in}(\omega)$ is smaller or equals the attenuation of $H_{mn}(\omega)$. Thus, the energy is still able to be focused on the original powered device. However, for the situation of $\theta_i < \theta_m$, the attenuation of $H_{in}(\omega)$ is larger than that of $H_{mn}(\omega)$. Thus, it is difficult to determine the comparison of $|H_{in}(\omega)|^2$ and $H_{mn}^*(\omega) H_{in}(\omega)$. In this circumstance, when the interference item is larger than the useful signal item, the energy from interference is the main item to control the power delivery direction, which makes focused signal useless. Even worse, it may lead unvalid of controlling the energy covered the whole frequency band focus on the powered devices.

Therefore, when all the devices are placed in the same plane, the energy can be only focused on the powered device with the largest elevation angle, which leads a lot of energy waste.

For addressing this problem and making the utmost of energy, here, we use a weight method to reduce the negative influence of interference on the useful focused signal.

First, let each powered device send charging request signal separately. And we record it at PSA, take time reversal, weight and channel compensation operation on it.

The processed signal can be wrote as

$$Y_{TR}^{m}(\omega) = \sum_{n=1}^{N} P_m^*(\omega) H_{mn}^*(\omega) F_n^*(\theta_m, \varphi_m, \omega) W_{mn}(\omega, \theta) \quad (11)$$

where $W_{mn}(\omega, \theta)$ is weight between the m^{th} powered device and the n^{th} antenna. This weight correlates to frequency and elevation angle, and can be expressed as

$$W_{mn}(\omega, \theta) = \frac{A_n(\theta)}{|H_{mn}(\omega)|} \quad (12)$$

$$A_n(\theta) = \int_0^{\frac{\pi}{2}} a_n(\theta_k) \otimes \delta(\theta - \theta_k) d\theta_k \quad (13)$$

where $A_n(\theta)$ is channel compensation between the n^{th} antenna and PRP with elevation angle θ, which is utilized to match the amplitude difference among channels, so that the interference from different elevation angles and channel difference can be suppressed. The value of $a_n(\theta_k)$ is reciprocal of channel gain between the n^{th} antenna and PRP with elevation angle θ_k. $\delta(\theta)$ is dirac function. The steps to obtain $W_{mn}(\omega, \theta)$ is as follows: 1) get the distance between PSA plane and PRP; 2) according to the models in IEEE802.15.3a, combined with the distance obtained in step 1), we can get channel gain in each path of each cluster. Then, the $A_n(\theta)$ is able to be deduced, and the weight $W_{mn}(\omega, \theta)$ can be calculated with the known channel information, which can be obtained by pre-test.

Next, we take the sum of all respective processed received charging request signals as excitation of corresponding antenna, by which all powered devices can be charged. The signal impinging on the i^{th} powered device is

$$\begin{aligned} Y_r(\theta_i, \varphi_i, \omega) &= \sum_{m=1}^{M} \sum_{n=1}^{N} P_m^*(\omega) H_{mn}^*(\omega) F_n^*(\theta_m, \varphi_m, \omega) \\ &\quad \times F_n(\theta_i, \varphi_i, \omega) W_{mn}(\omega, \theta_i) H_{in}(\omega) \\ &= \underbrace{\sum_{n=1}^{N} P_i^*(\omega) |H_{in}(\omega)| |F_n(\theta_i, \varphi_i, \omega)|^2 A_n(\theta_i)}_{\text{useful signal}} \\ &\quad + \underbrace{\sum_{\substack{m=1 \\ m \neq i}}^{M} \sum_{n=1}^{N} P_m^*(\omega) \frac{H_{mn}^*(\omega)}{|H_{mn}(\omega)|}}_{\text{interference}} \\ &\quad \underbrace{\times F_n^*(\theta_m, \varphi_m, \omega) F_n(\theta_i, \varphi_i, \omega) H_{in}(\omega) A_n(\theta_i)}_{\text{interference}} \end{aligned} \quad (14)$$

Similarly, the signal impinging on other places (θ_x, φ_x), where $\theta_x \subseteq [0, \frac{\pi}{2}]$, $\varphi_x \subseteq [0, 2\pi)$ ($\theta_x \neq \theta_m$ or $\varphi_x \neq \varphi_m$) is

$$\begin{aligned} Y_r(\theta_x, \varphi_x, \omega) &= \sum_{m=1}^{M} \sum_{n=1}^{N} P_m^*(\omega) H_{mn}^*(\omega) F_n^*(\theta_m, \varphi_m, \omega) \\ &\quad \times F_n(\theta_x, \varphi_x, \omega) W_{mn}(\omega, \theta_x) H_{xn}(\omega) \\ &= \sum_{m=1}^{M} \sum_{n=1}^{N} P_m^*(\omega) \frac{H_{mn}^*(\omega)}{|H_{mn}(\omega)|} F_n^*(\theta_m, \varphi_m, \omega) \\ &\quad \times F_n(\theta_x, \varphi_x, \omega) H_{xn}(\omega) A_n(\theta_x) \end{aligned} \quad (15)$$

It can be seen from eq.(14), $|H_{in}(\omega)| > H_{in}(\omega) \frac{H_{mn}^*(\omega)}{|H_{mn}(\omega)|}$, and $|F_n(\theta_i, \varphi_i, \omega)|^2 > F_n^*(\theta_m, \varphi_m, \omega) F_n(\theta_i, \varphi_i, \omega)$ is always true for omnidirectional antennas. Thus, we can conclude that the focused useful signal item is always greater than interference item. Further, the focused useful signal, which is always towards the corresponding powered device, is the main item to control the power delivery direction. Therefore, this proposed method can control the power covered the whole frequency band focus on the corresponding powered devices, which make the energy use most. It is also proved that this proposed method can achieve power focus over the whole frequency band with only one-time TR operation and Fourier transformation, which is a simple method.

Moreover, compare eq.(14) with eq.(15), the advantages of introducing weight can be summarized as two aspects: one is the power impinging on multi-powered devices is almost the same; the other one is making $|H_{xn}(\omega) A_n(\theta_x)| \approx |H_{in}(\omega) A_n(\theta_i)|$. Thus, $|H_{in}(\omega)| A_n(\theta_i) > H_{xn}(\omega) A_n(\theta_x) \frac{H_{mn}^*(\omega)}{|H_{mn}(\omega)|}$, then $Y_r(\theta_i, \varphi_i, \omega)$ is always greater than $Y_r(\theta_x, \varphi_x, \omega)$. Namely, the power impinging on the powered device is always greater than that arriving at other places in the PRP, which enhances the PCE and reduces the waste of energy.

Here, we give the expression of PCE in the m^{th} powered device as

$$PCE_m \triangleq \frac{P_{d_m}}{P_L} = \frac{|Y_r(\omega, \theta_m, \varphi_m)|^2}{\int_{\theta,\varphi} |Y_r(\omega, \theta, \varphi)|^2 d\theta d\varphi} \quad (16)$$

where, P_{d_m} represents the power impinging on the m^{th} powered device, and P_L denotes the power impinging on the PRP with fixed θ or ϕ. Therein, ϕ is changed when θ is fixed, and vice versa.

III. RESULTS AND DISCUSSION

In this section, we simulate WPT in a 3D indoor environment based on the non-line of sight model in IEEE 802.15.3a by the proposed method and algorithm, whose performance is compared with those obtained by just taking TR operation and sending power directly.

We take modulated gaussian pulse centered at 2.45 GHz with 3 ns duration as charging request signal of all powered devices. By only single run of TR operation and Fourier transformation, the wideband excitation is achieved by the proposed algorithm presented above. The advantage of wideband can be concluded that wideband excitation make this proposed WPT method suitable for many applications, since many electric devices for specific applications have their own work bands, when the wideband exciation covers their work bands, they can be charged in low battery status whatever the kind of them is.

Here, the PSA can be constructed by different number of omnidirectional antennas with different arrangement. Although, the arrangement of PSA can be generated randomly, it must obey the designed principles. That is according to the common design of antennas, the size of antenna worked at 2.45 GHz is about $\lambda/4 = 30.6$ mm, and the distance between each antenna element is at least $\lambda/2 = 61.2$ mm in order to avoid the interference among each antenna, which is designed based on antenna theory [36]. In the following simulations, the total number of antenna is N = 48 and 80 respectively, and the PSA is fixed on the ceiling. The center of ceiling is chosen as the center of PSA. In N = 48 case, N = N1 × N2 = 8 column × 6 line. And in N = 80 case, N = N1 × N2 = 10 column × 8 line, where N1 is the number of antennas in column, and N2 is the number of antennas in line.

According to the general structure of room, we assume the size of ceiling and ground are both 15×10 m^2, and the height of room is L = 3 m, which is used as the distance between ceiling and PRP in the first and third simulation. Therein, the first simulation is used to explore the performance of the proposed method on WPT for three devices placed arbitrarily in the same PRP, the second simulation is utilized to study the affect of different PRPs on the performance of proposed method, where L is changed into L1 = 2.5 m for device 1, L2 = 2 m for device 2 and L3 = 1.5 m for device 3 without changing the positions of three devices compared with the first simulation, and the third simulation is executed to invest the performance of the proposed method on WPT for gathering three devices at the corner of PRP, where three devices are also put in the same PRP, since the distance between each device is smallest when they are placed in the same plane.

Moreover, our simulations are all executed by an Intel Core i7-7500U CPU, 8G RAM laptop. The step of observation angles is 5°, which is the smallest step based on the memory of laptop. The ranges of observation azimuth angle and elevation angle are respectively [0°, 360°] and [0°, 90°]. Thus, we can define the device's position as $\theta_{device} = 0° + z_\theta \times 5°$ for elevation angle of device and $\phi_{device} = 0° + z_\phi \times 5°$ for azimuth angle of device, where $z_\theta \in [0, 18]$ and $z_\phi \in [0, 72]$ are both positive integer. In the first and second simulation, we choose $z_\theta = 4$ and $z_\phi = 24$ for device 1 ($\theta_1 = 20°$, $\varphi_1 = 120°$ in polar coordinate, and ($x_{device1} = Lcot(\theta_1)cos(\phi_1)$, $y_{device1} = Lcot(\theta_1)sin(\phi_1)$) = (-4.12 m, 7.14 m) in the orthogonal coordinate), $z_\theta = 10$ and $z_\phi = 18$ for device 2 ($\theta_2 = 50°$, $\varphi_2 = 90°$ in polar coordinate, and ($x_{device2} = Lcot(\theta_2)cos(\phi_2)$, $y_{device2} = Lcot(\theta_2)sin(\phi_2)$) = (2.52 m, 0 m) in the orthogonal coordinate), and $z_\theta = 12$ and $z_\phi = 8$ for device 3 ($\theta_3 = 60°$, $\varphi_3 = 40°$ in polar coordinate, and ($x_{device3} = Lcot(\theta_3)cos(\phi_3)$, $y_{device3} = Lcot(\theta_3)sin(\phi_3)$) = (1.11 m, 1.33 m) in the orthogonal coordinate). Thus, we can get the distances between each powered device are respectively $|r_{device1} - r_{device2}| = \sqrt{(x_{device1} - x_{device2})^2 + (y_{device1} - y_{device2})^2} = 9.74$ m, $|r_{device1} - r_{device3}| = 7.82$ m, and $|r_{device2} - r_{device3}| = 1.92$ m.

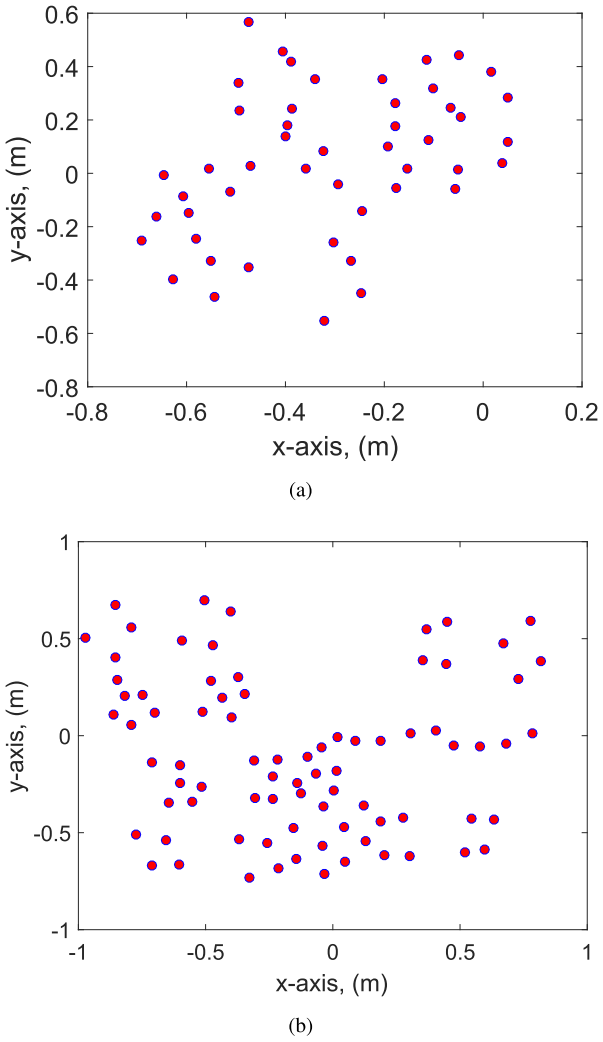

FIGURE 2. The arrangement of PSA. (a) N = 48; (b) N = 80.

Fig.2 shows one kind of PSA's antenna arrangement, which is produced randomly and obey our design principle. The analyses below are all based on these two arrangements. Note the distance between each antenna is on the order of centimeter. Therefore, some of antennas' positions look very close in Fig.2 with the order of meter.

The signal strengths observed at respective PRP in N = 48 and N = 80 cases are separately shown in Fig.3 and Fig.4, which are polar diagrams in the respective radiation plane. It can be seen clearly that the main pattern is just at $\theta = 90°$ in sending power directly case, and with the increasement of N, the main pattern is more focused and sidelobes are smaller. In just taking TR operation case, the signal pattern is towards the directions of three devices with large beamwidth compared with those obtained in proposed method case. Also, with the increasement of N, the signal pattern is more focused and beamwidths become narrower. While, in proposed method case, the narrow beamwidths can be always got whenever N = 48 and N = 80.

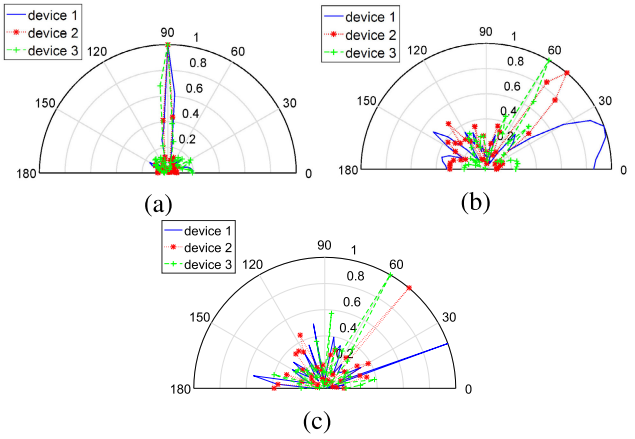

FIGURE 3. The signal pattern observed at PRP, when PSA consists of 48 antennas. Therein, observation azimuth angle $\phi = 120°$ and $300°$ for device 1, $\phi = 90°$ and $270°$ for device 2, $\phi = 40°$ and $220°$ for device 3. (a) By sending power directly, (b) by just taking TR operation, (c) by proposed method.

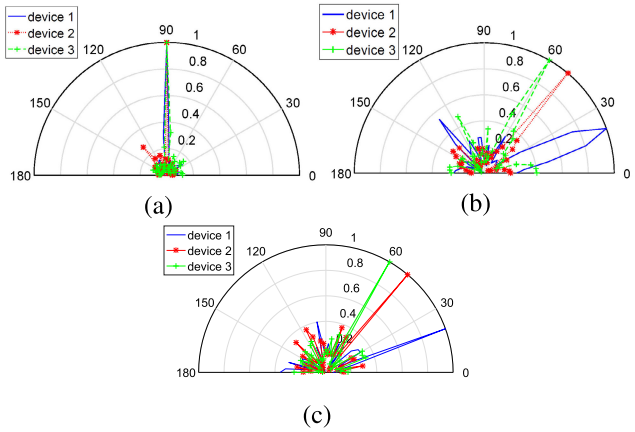

FIGURE 4. The signal pattern observed at PRP, when PSA consists of 80 antennas. Therein, observation azimuth angle $\phi = 120°$ and $300°$ for device 1, $\phi = 90°$ and $270°$ for device 2, $\phi = 40°$ and $220°$ for device 3. (a) By sending power directly, (b) by just taking TR operation, (c) by proposed method.

Thus, the proposed method can provide the precise power delivery towards powered devices, and does not make the interference to non-powered devices even with small N. Besides, the sidelobes in non-powered devices' directions become weaker with the increasement of N. Thus, there are more power impinging on the powered devices, which can also be proved in normalization power maps generated by 48 and 80 antennas respectively shown in Figs.5 and 6.

By sending power directly, the power arriving at the three powered devices are very small whenever N = 48 or N = 80 as shown in Figs. 5(a) and 6(a). Therefore, sending power directly is not a suitable method for powering multi-kind/multi device placed arbitrarily. By just taking TR operation as shown in Figs. 5(b) and 6(b), although three powered devices can be charged, the sidelobes are high, which leads to a large interference to non-power devices, especially the one near the powered device. This situation can be alleviated

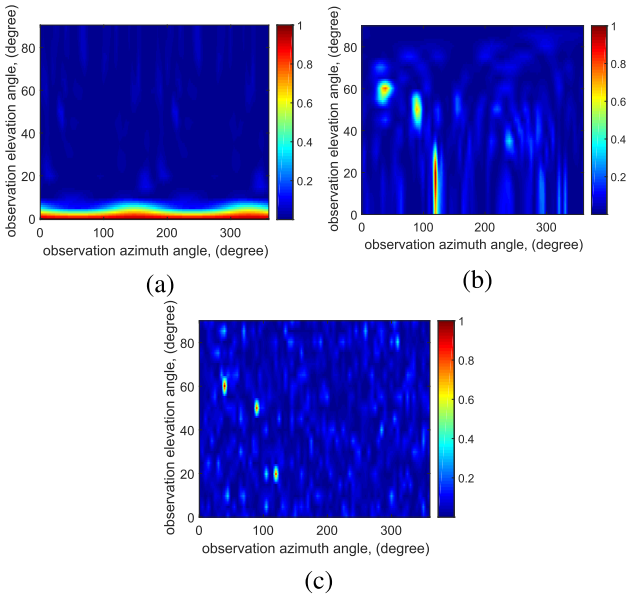

FIGURE 5. When PSA consists of 48 antennas, the power map of PRP obtained by (a) sending power directly, (b) just taking TR operation, (c) proposed method.

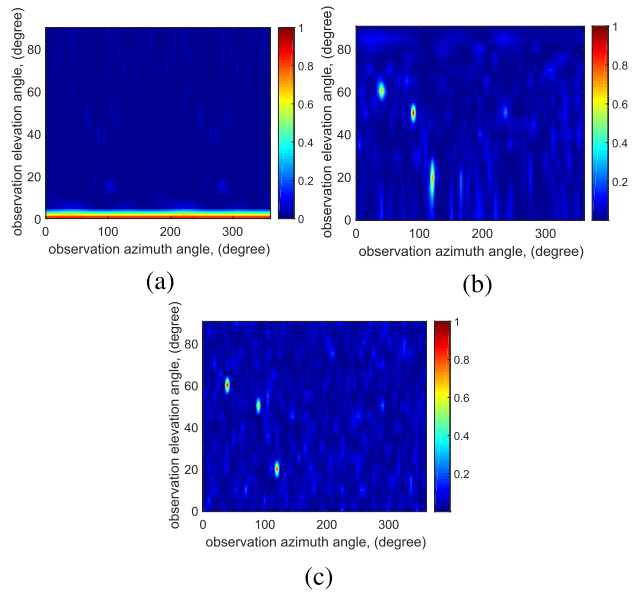

FIGURE 6. When PSA consists of 80 antennas, the power map of PRP obtained by (a) sending power directly, (b) just taking TR operation, (c) proposed method.

by increasing N. Namely, the sidelobes or the interference to non-powered devices can be improved with the increasement of N. However, by the proposed method, the three powered devices can be charged effectively. The power arriving at the powered devices are much more than those arriving at non-powered devices' positions, especially the near one. Also the power obtained by powered devices are increased by increasing N as shown in Figs. 5(c) and 6(c). The most obvious difference between N = 48 case and N = 80 case

TABLE 1. Comparison of the proposed method, just taking TR operation and sending power directly.

Case/Description			The proposed method		Just taking TR operation		Sending power directly	
			N=48	N=80	N=48	N=80	N=48	N=80
PCE	Three powered devices in the same PRP (L=3m)	Device 1 in θ plane	55.65%	61.4%	13.7%	21.91%	0.98%	0.43%
		Device 2 in θ plane	55.55%	60.56%	33.34%	68.73%	0.42%	0.018%
		Device 3 in θ plane	45.83%	56.96%	48.31%	54.61%	0.89%	1.13%
		Device 1 in ϕ plane	18.52%	24.26%	22.03%	24.46%	1.79%	0.6%
		Device 2 in ϕ plane	19.12%	21.17%	12.02%	23.06%	0.84%	0.035%
		Device 3 in ϕ plane	22.44%	27.71%	14.4%	24.57%	1.92%	4.63%
PCE	Three powered devices in different PRPs L1=2.5 m (device 1), L2=2m (device 2), L3=1.5m (device3)	Device 1 in θ plane	18.76%	30.37%	1.34%	7.31%	1.34%	0.59%
		Device 2 in θ plane	44.92%	53.37%	43.51%	73.37%	0.84%	0.035%
		Device 3 in θ plane	67.4%	67.2%	34.8%	66.88%	2.65%	2.26%
		Device 1 in ϕ plane	19.33%	24.33%	1.62%	6.21%	2.45%	0.82%
		Device 2 in ϕ plane	14.34%	26.66%	20.42%	35%	1.67%	0.069%
		Device 3 in ϕ plane	21.4%	21.63%	10.9%	23%	3.84%	11.75%
Sidelobe (interference to other electronic devices)			Small		Big		Small	
Whether power multi-kind/multi electronic devices or not			Yes		Yes		No	
Whether the unfairness is addressed or not			Yes		No		No	

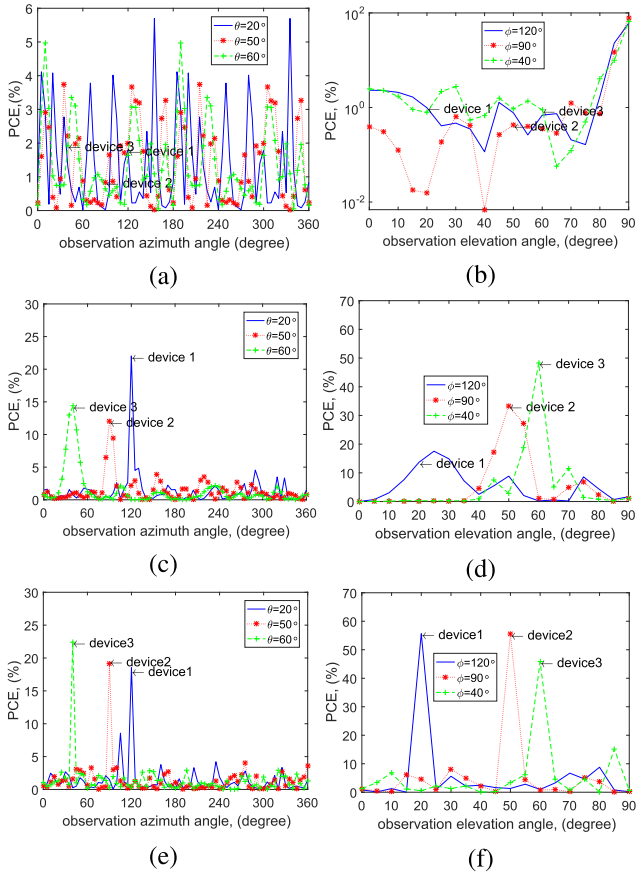

FIGURE 7. When PSA consists of 48 antennas, the PCE observed at PRP versus: (a) azimuth angle in sending power directly case; (b) elevation angle in sending power directly case; (c) azimuth angle in just taking TR operation case; (d) elevation angle in just taking TR operation case; (e) azimuth angle in proposed method case; (f) elevation angle in proposed method case.

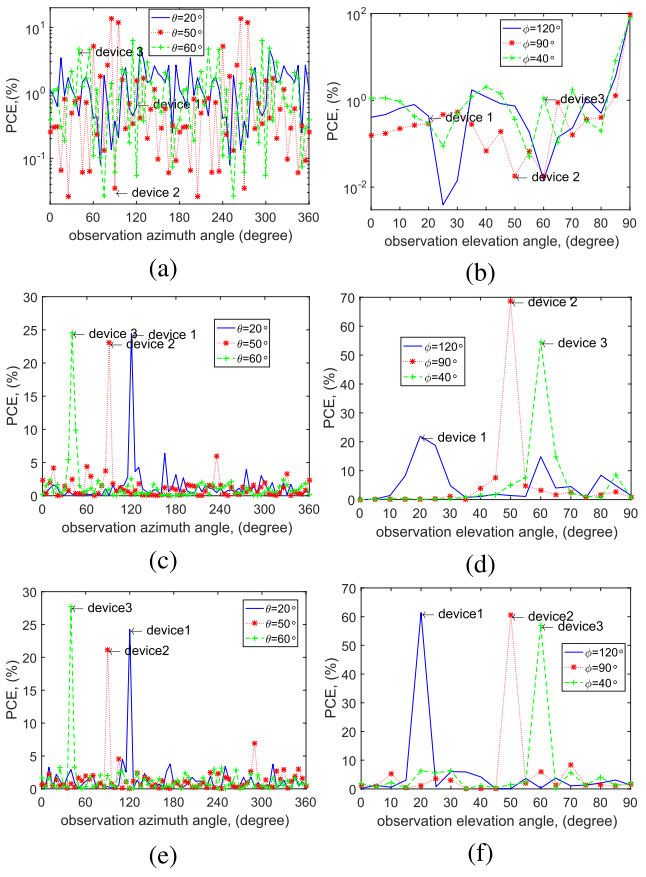

FIGURE 8. When PSA consists of 80 antennas, the PCE observed at PRP: (a) azimuth angle in sending power directly case; (b) elevation angle in sending power directly case; (c) azimuth angle in just taking TR operation case; (d) elevation angle in just taking TR operation case; (e) azimuth angle in proposed method case; (f) elevation angle in proposed method case.

is that the PCE obtained in N = 80 case is larger, since the power from the PSA is larger in N = 80 case than that in N = 48 case, which can also be proved in the research of PCE as shown in Figs. 7 and 8.

Figs.7 and 8 show the PCE observed at observation azimuth angle (ϕ) plane and elevation angle (θ) plane of each device. The exact value of PCE is shown in Table 1. It can be seen clearly that by sending power directly, the power can

not be received by these three powered devices effectively whether in N = 48 case and N = 80 case, the PCEs are very low just smaller than 2% in N = 48 case and 5% in N = 80 case. Additionally, the PCEs of device 1 and device 2 are larger in N = 48 case than those in N = 80 case in both θ and ϕ planes, since larger N leads to a narrower or more focused signal pattern in $\theta = 90°$ (shown in Figs 3(a) and 4(a)) and the θ for device 1 and device 2 are respectively 20° and 50°, which is far away from $\theta = 90°$. Unlikely, the θ for device 3 is near 90°, thus, the PCEs for device 3 in N = 80 case are larger than those in N = 48 case in both θ and ϕ planes.

Compared with the method of sending power directly, just taking TR operation and the proposed method can enhance PCE greatly. While the PCEs of three powered devices obtained by just taking TR operation are quite different among each other, which is called unfairness of power. Specifically, the biggest differences are separately more than 34% and 45% in θ plane in N = 48 case and N = 80 case, and more than 10% in ϕ plane in N = 48 case, although the PCEs in ϕ plane in N = 80 case is almost the same.

Fortunately, the unfairness is alleviated by the proposed method. Specifically, the biggest differences are separately less than 5% and 4% in θ plane in N = 48 case and N = 80 case, and 4% in ϕ plane in both N = 48 and N = 80 cases. Thus, we can conclude the efficiency and unfairness of power are improved by the proposed methods, even in the condition that three devices are placed in different PRPs, which is the second simulation. Its PCE values are shown in Table 1 as well. The small difference among the values of PCE in the same case is introduced by different channel information. Furthermore, the PCE is enhanced whether in azimuth angle or elevation angle with the increasement of N. Thus, we can conclude that PCE can be improved further by properly increasing the number of antennas. By the way, we found the PCE of powered device is sometimes greater in just taking TR operation case than that obtained by proposed method. That is because the power from PSA is limited and quantitative, and if the most of this power is focused on one place, the other places will get little power, which also generates power unfairness problem. Thus, although some powered devices can obtain more power in just taking TR operation, this method is not suitable for charging multi-device because of power unfairness.

In the second simulation, although these three devices are positioned in different planes, they can be powered effectively with small sidelobes as shown in Figs.9 and 11, which means the interference to non-powered devices is small. However, three devices are not able to be charged simultaneously by just taking TR operation, and can not be charged at all by sending power directly as the PCE values shown in Table 1. Thus, the proposed method can be used to charge devices effectively in different planes in a 3D indoor environment. Besides, although the different PRPs do affect the PCEs in θ plane as shown in Figs.10(b) and 12(b), since the elevation angle θ is the main factor affected by the different distances between PRPs and PSA plane, the unfairness of power in

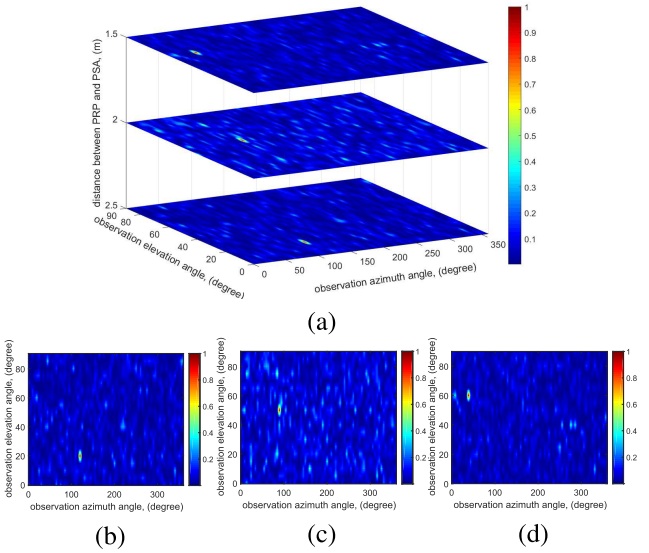

FIGURE 9. When PSA consists of 48 antennas, the power observed at respective PRP: (a) in a 3D indoor environment; (b) device 1 in L1 plane; (c) device 2 in L2 plane; (d) device 3 in L3 plane.

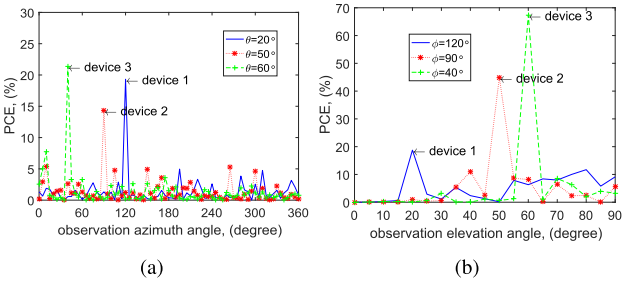

FIGURE 10. When PSA consists of 48 antennas, the observed PCE at respective PRP generated by proposed method. (a) azimuth angle; (b) elevation angle.

θ plane is still better than that obtained by just taking TR operation. Moreover, the unfairness of power in ϕ plane is addressed as shown in Figs.10(a) and 12(a), which is similar as the first simulation, since the different PRPs have little influence on PCEs in ϕ plane, which is quite different from the situation in θ plane.

In the last simulation, we gather three devices at the corner of the same PRP (L = 3m). According to the size of room, we can get the elevation angle of corner is $arctan(3/\sqrt{(15/2)^2 + (10/2)^2}) = 18.41°$, and the azimuth angle of corner is $arctan(\frac{10/2}{15/2}) = 33.69°$. We choose the elevation angle of corner as $\theta = 20°$ and the azimuth angle of corner as $\phi = 35°$ according to the simulation step. One device is put at the corner, namely, $z_\theta = 4$ and $z_\phi = 7$ for the device 1 ($\theta_1 = 20°$, $\phi_1 = 35°$ in the polar coordinate, $(x_{device1} = Lcot(\theta_1)cos(\phi_1), y_{device1} = Lcot(\theta_1)sin(\phi_1)) = (4.73\text{ m}, 6.75\text{ m})$ in the orthogonal coordinate), the other two devices are put around device 1. Here, at least one of θ and ϕ is unchanged for obtaining the smallest distance between each device, and we choose θ unchanged for example. Namely, $z_\theta = 4$ and $z_\phi = 6$ for the device 2 ($\theta_1 = 20°$, $\phi_1 = 30°$ in the polar coordinate,

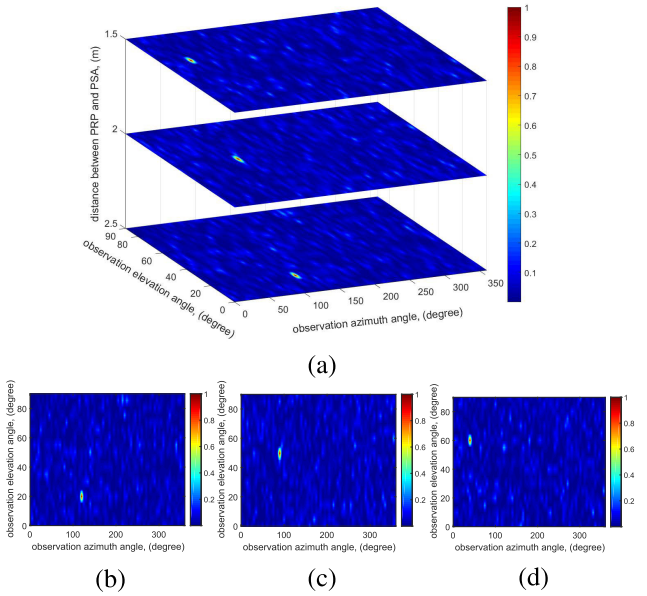

FIGURE 11. When PSA consists of 80 antennas, the power observed at respective PRP: (a) in a 3D indoor environment; (b) device 1 in L1 plane; (c) device 2 in L2 plane; (d) device 3 in L3 plane.

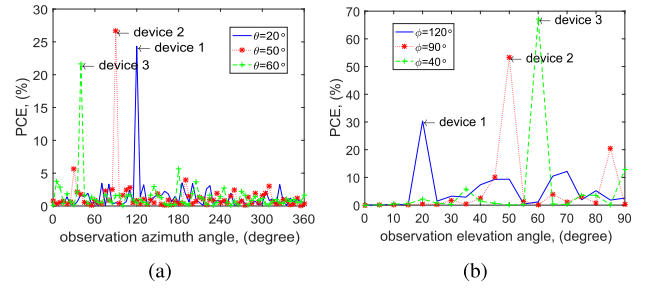

FIGURE 12. When PSA consists of 80 antennas, the observed PCE at respective PRP generated by proposed method. (a) azimuth angle; (b) elevation angle.

$(x_{device2} = Lcot(\theta_2)cos(\phi_2), y_{device2} = Lcot(\theta_2)sin(\phi_2)) =$ (4.12 m, 7.14 m) in the orthogonal coordinate), and $z_\theta = 4$ and $z_\phi = 8$ for the device 3 ($\theta_3 = 20°, \phi_3 = 40°$ in the polar coordinate, $(x_{device3} = Lcot(\theta_3)cos(\phi_3), y_{device3} = Lcot(\theta_3)$ $sin(\phi_3)) =$ (5.30 m, 6.31 m) in the orthogonal coordinate). Then, we can get that the distances between each device are separately $|r_{device1} - r_{device2}| = 0.72$ m, $|r_{device1} - r_{device3}| =$ 0.72 m, and $|r_{device2} - r_{device3}| = 1.44$ m. Thus, the distance step is 0.72 m.

The power map and PCE observed at PRP in N = 48 case and N = 80 case are shown in Figs.13 and 14 respectively. It can be seen clearly that whenever in N = 48 case and N = 80 case, these three powered devices can be all powered effectively. The power and PCE arriving at non-powered devices are very low compared with those in the powered devices' positions. Especially, it is much clearer in the extended figures as Figs. 13(b) and 14(b) shown, the power is just focused in the powered devices' locations, and decreases fast at non-powered devices even when the non-powered devices are near the powered devices. Thus, the interference to non-powered devices is suppressed effectively by the proposed method, which can be also proved in the PCE results

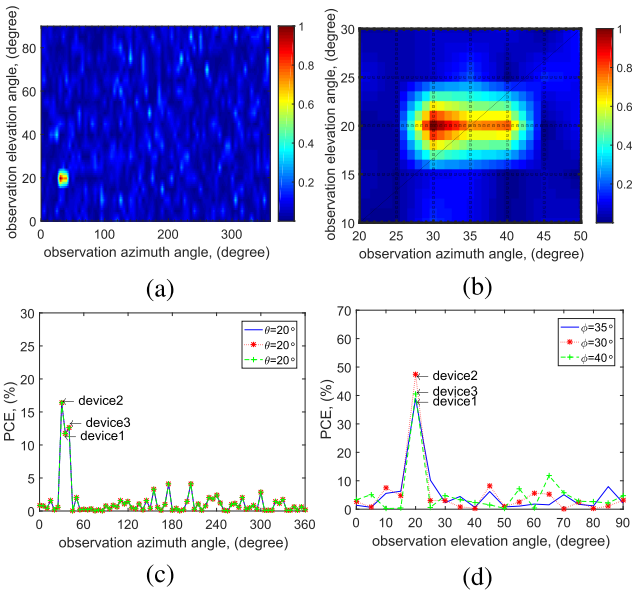

FIGURE 13. When PSA consists of 48 antennas, the power and PCE observed at PRP (L = 3 m): (a) power map; (b) the extended power map; (c) PCE versus azimuth angle; (d) PCE versus elevation angle.

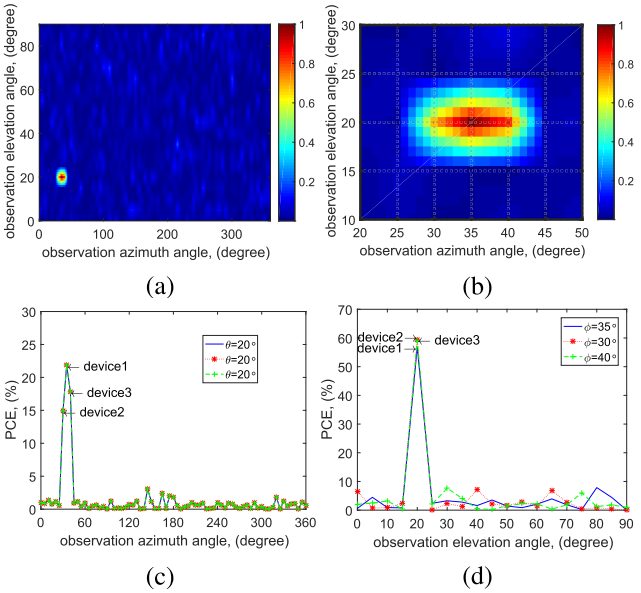

FIGURE 14. When PSA consists of 80 antennas, the power and PCE observed at PRP (L = 3 m): (a) power map; (b) the extended power map; (c) PCE versus azimuth angle; (d) PCE versus elevation angle.

as shown in Figs. 13(c)(d) and 14(c)(d). Because these three devices have the same θ, the curves of PCE versus azimuth angle are the same as shown in Figs. 13(c) and 14(c), and the PCEs of these three powered devices are obviously larger than those observed at non-powered devices. Besides, the same results can be obtained in the result of PCE versus elevation angle as shown in Figs. 13(d) and 14(d). Furthermore, compared Fig. 13 with Fig. 14, we can conclude that the power map and PCE are more focused on the powered devices with the increasement of N. It is worth mention that the ability of focusing power towards the powered devices of our proposed method can not be affected negatively by changing

the number of antennas. In other words, the sidelobes can be suppressed effectively in both N = 48 case and N = 80 case.

Besides, all simulations consider the equipments hoped to construct the measurement. Our algorithm of processing signal including TR and weight operations can be executed in the traditional computer. And the receiving charging request signal can be recorded by the traditional digital serial analyzer such as Tektronix DSA 72004B. The excitation signal can be generated and delivered to PSA by the traditional arbitrary waveform generator such as Agilent AWG 7122B. It can be seen that the equipments used in this WPT can be very common and have been put into use for many years. Thus, our scheme is feasible and not complex. Furthermore, the PCE is discussed on the premise that the power from PSA is 100%. In the actual application, the total efficiency can be obtained just through multiplying this PCE by the efficiency of used equipment, which is easy to implement.

Additionally, we want to explain the reason why we use omni-directional antenna elements to build PSA. We can image that if we use directional antenna elements instead of omni-directional antenna elements to construct PSA, some places in the PRP can obtained much power, while, other places in the PRP can receive seldom power, which will lead to a more serious power unfairness problem. Thus, the omni-directional antenna element is the best choice.

As we known, the simulations are both on the conditions of N = 48 and N = 80. But, there is no criterion for choosing N. It can be designed according to your applications, such as the wanted PCE, the size of indoor environments and the size of ceiling. If the N is small, such as 10 or 20, the PCE will be small compared with the data in this paper. But, the focusing property to the wanted places is still work.

IV. CONCLUSION

In this paper, we propose a method and algorithm to charge multi-kind/multi powered devices wirelessly and simultaneously in 3D indoor environments. Different from those methods used in WPT, such as beamforming and retro-reflection, the wideband excitation can be achieved by one-time TR operation and Fourier transformation, which avoids complex single frequency optimization in conventional WPT. The basic physical idea of our method is utilizing the auto-match of antenna radiation and environment adaptability of TR. This principle allows us to focus the power only towards the directions of powered devices, which is not interference to non-powered devices. Besides, this method is suitable for the condition of using omnidirectional antennas with any structure and arrangement as PSA, which breaks the limitations of antenna structure and arrangement in conventional WPT. Additionally, the proposed method also address the power unfairness problem, which usually happens in charging multi-powered devices. The potential applications of our proposed method is not limited to the indoor environments, and is also able to be used in complex media for outdoor environment.

REFERENCES

[1] F. Lu, H. Zhang, C. Zhu, L. Diao, M. Gong, W. Zhang, and C. C. Mi, "A tightly coupled inductive power transfer system for low-voltage and high-current charging of automatic guided vehicles," *IEEE Trans. Ind. Electron.*, vol. 66, no. 9, pp. 6867–6875, Sep. 2019.

[2] S. Lee, G. Jung, S. Shin, Y. Kim, B. Song, J. Shin, and D. Cho, "The optimal design of high-powered power supply modules for wireless power transferred train," in *Proc. Elect. Syst. Aircr., Railway Ship Propuls.*, Oct. 2012, pp. 1–4.

[3] R. Das, A. Basir, and H. Yoo, "A metamaterial-coupled wireless power transfer system based on cubic high-dielectric resonators," *IEEE Trans. Ind. Electron.*, vol. 66, no. 9, pp. 7397–7406, Sep. 2019.

[4] H. Qian, P. Zhou, C. Wang, Y. Deng, and G. Ma, "Wireless power supply for HTS magnets: Circuit topology design and cryogenic testing," *IEEE Trans. Appl. Supercond.*, vol. 29, no. 5, Aug. 2019, Art. no. 4602205.

[5] Y. D. Chung, C. Y. Lee, W. S. Lee, and E. Y. Park, "Operating characteristics for different resonance frequency ranges of wireless power charging system in superconducting MAGLEV train," *IEEE Trans. Appl. Supercond.*, vol. 29, no. 5, Aug. 2019, Art. no. 3602405.

[6] D. Shi, L. Zhang, H. Ma, Z. Wang, Y. Wang, and Z. Cui, "Research on wireless power transmission system between satellites," in *Proc. IEEE Wireless Power Transf. Conf.*, May 2016, pp. 1–4.

[7] Z. Lin, M. Lin, J. Ouyang, W.-P. Zhu, and S. Chatzinotas, "Beamforming for secure wireless information and power transfer in terrestrial networks coexisting with satellite networks," *IEEE Signal Process. Lett.*, vol. 25, no. 8, pp. 1166–1170, Aug. 2018.

[8] C. Bergsrud, S. Noghanian, J. Straub, D. Whalen, and R. Fevig, "Orbit-to-ground wireless power transfer test mission," in *Proc. IEEE Aerosp. Conf.*, Mar. 2013, pp. 1–11.

[9] J. Xu, Y. Zeng, and R. Zhang, "UAV-enabled wireless power transfer: Trajectory design and energy optimization," *IEEE Trans. Wireless Commun.*, vol. 17, no. 8, pp. 5092–5106, Aug. 2018.

[10] D. Arnitz and M. S. Reynolds, "Multitransmitter wireless power transfer optimization for backscatter RFID transponders," *IEEE Antennas Wireless Propag. Lett.*, vol. 12, pp. 849–852, 2013.

[11] E. Moradi, L. Sydänheimo, G. S. Bova, and L. Ukkonen, "Measurement of wireless power transfer to deep-tissue RFID-based implants using wireless repeater node," *IEEE Antennas Wireless Propag. Lett.*, vol. 16, pp. 2171–2174, 2017.

[12] W. Zhou, S. Sandeep, P. Wu, P. Yang, W. Yu, and S. Y. Huang, "A wideband strongly coupled magnetic resonance wireless power transfer system and its circuit analysis," *IEEE Microw. Wireless Compon. Lett.*, vol. 28, no. 12, pp. 1152–1154, Dec. 2018.

[13] J.-P. Curty, N. Joehl, C. Dehollain, and M. J. Declercq, "Remotely powered addressable UHF RFID integrated system," *IEEE J. Solid-State Circuits*, vol. 40, no. 11, pp. 2193–2202, Nov. 2005.

[14] A. Kurs, A. Karalis, R. Moffatt, J. D. Joannopoulos, P. Fisher, and M. Soljačić, "Wireless power transfer via strongly coupled magnetic resonances," *Science*, vol. 317, no. 5834, pp. 83–86, 2007.

[15] J. Wang, M. Leach, E. G. Lim, Z. Wang, and Y. Huang, "Investigation of magnetic resonance coupling circuit topologies for wireless power transmission," *Microw. Opt. Technol. Lett.*, vol. 61, no. 7, pp. 1755–1763, 2019.

[16] A. M. Jawad, R. Nordin, S. K. Gharghan, H. M. Jawad, and M. Ismail, "Opportunities and challenges for near-field wireless power transfer: A review," *Energies*, vol. 10, no. 7, p. 1022, 2017.

[17] B. Li, B.-J. Hu, X. Li, M. Deng, and Z.-H. Wei, "Efficiency enhancement of long-distance wireless power transmission using time reversal technique," in *Proc. IEEE Int. Conf. Comput. Electromagn.*, Feb. 2016, pp. 49–51.

[18] J. O. McSpadden and J. C. Mankins, "Space solar power programs and microwave wireless power transmission technology," *IEEE Microw. Mag.*, vol. 3, no. 4, pp. 46–57, Dec. 2002.

[19] G. Franceschetti, "The new scientific scenario of power wireless transmission," in *Proc. IEEE Antennas Propag. Soc. Int. Symp.*, Jul. 2010, p. 1.

[20] Y. Alsaba, S. K. A. Rahim, and C. Y. Leow, "Beamforming in wireless energy harvesting communications systems: A survey," *IEEE Commun. Surveys Tuts.*, vol. 20, no. 2, pp. 1329–1360, 2nd Quart., 2018.

[21] Z. Wang, L. Duan, and R. Zhang, "Adaptively directional wireless power transfer for large-scale sensor networks," *IEEE J. Sel. Areas Commun.*, vol. 34, no. 5, pp. 1785–1800, May 2016.

[22] Y. Lim and J. Park, "A novel phase-control-based energy beamforming techniques in nonradiative wireless power transfer," *IEEE Trans. Power Electron.*, vol. 30, no. 11, pp. 6274–6287, Nov. 2015.

[23] Q. Shi, W. Xu, J. Wu, E. Song, and Y. Wang, "Secure beamforming for MIMO broadcasting with wireless information and power transfer," *IEEE Trans. Wireless Commun.*, vol. 14, no. 5, pp. 2841–2853, May 2015.
[24] H. Zhai, H. K. Pan and M. Lu, "A practical wireless charging system based on ultra-wideband retro-reflective beamforming," in *Proc. IEEE Antennas Propag. Soc. Int. Symp.*, Jul. 2010, pp. 1–4.
[25] S. Bi, C. K. Ho, and R. Zhang, "Wireless powered communication: Opportunities and challenges," *IEEE Commun. Mag.*, vol. 53, no. 4, pp. 117–125, Apr. 2015.
[26] S. Ding, Y. Fang, J.-F. Zhu, Y. Yang, and B.-Z. Wang, "Wireless cloaking system based on time-reversal multipath propagation effects," *IEEE Trans. Antennas Propag.*, vol. 67, no. 2, pp. 1386–1391, Feb. 2019.
[27] W. Lei and L. Yao, "Performance analysis of time reversal communication systems," *IEEE Commun. Lett.*, vol. 23, no. 4, pp. 680–683, Apr. 2019.
[28] B. Li and B.-J. Hu, "Time reversal based on noise suppression imaging method by using few echo signals," *IEEE Antennas Wireless Propag. Lett.*, vol. 14, pp. 12–15, 2014.
[29] B. Li, S. Liu, D. Zhao, and B.J. Hu, "DOA estimation of unknown emitter signal based on time reversal and coprime array," *Sensors*, vol. 19, no. 6, p. 1398, 2019.
[30] D. Zhao and M. Zhu, "Generating microwave spatial fields with arbitrary patterns," *IEEE Antennas Wireless Propag. Lett.*, vol. 15, pp. 1739–1742, 2016.
[31] M. Fink, "Time reversed acoustics," *Phys. Today*, vol. 50, no. 3, pp. 34–40, 1997.
[32] G. Lerosey, J. de Rosny, A. Tourin, A. Derode, G. Montaldo, and M. Fink, "Time reversal of electromagnetic waves," *Phys. Rev. Lett.*, vol. 92, no. 19, p. 193904, May 2004.
[33] Z. Nie and Y. Yang, "A model independent scheme of adaptive focusing for wireless powering to in-body shifting medical device," *IEEE Trans. Antennas Propag.*, vol. 66, no. 3, pp. 1497–1506, Mar. 2018.
[34] J. R. Foerster, *Channel Modelling Sub-Committee Report Final*, IEEE Standard P802.1502/490rl SG3a, 2003.
[35] E. M. Shaheen and M. El-Tanany, "The impact of narrowband interference on the performance of UWB systems in the IEEE802.15.3a channel models," in *Proc. CCECE*, May 2010, pp. 1–6.
[36] W. L. Stutzman and G. A. Thiele, *Antenna Theory and Design*, 2nd ed. Hoboken, NJ, USA: Wiley, 1998, pp. 87–135.

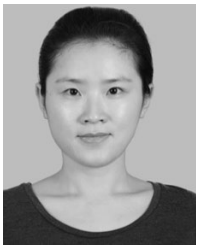

BING LI received the B.S. degree in electronic information science and technology and the M.S. degree in radio physics from the University of Electronic Science and Technology of China (UESTC), Chengdu, China, in 2010 and 2013, respectively, and the Ph.D. degree in information and communication engineering from the South China University of Technology (SCUT), Guangzhou, China, in 2016.

She is currently a Lecturer with the School of Electrical Engineering, Southwest Jiaotong University (SWJTU), Chengdu. She is also a Postdoctoral with the School of Physics, University of Electronic Science and Technology of China (UESTC). She is also a postdoctoral with the Institut Langevin, Paris, France. Her research interests include the time reversal method, imaging method, non-destructive damage detection, wireless power transmission, antennas, and radio technology.

SHIQI LIU received the B.S. degree in electronic and information engineering from the Wuhan University of Science and Technology, Wuhan, in 2009, and the Ph.D. degree in information and communication engineering from the South China University of Technology (SCUT), Guangzhou, in 2014.

He is currently a Postdoctoral Research Associate with the Guangdong Key Laboratory of Intelligent Information Processing, College of Information Engineering, Shenzhen University, Shenzhen, China. He is also a Senior Engineer with the Southwest China Research Institute of Electronic Equipment. His research interests include wireless communications, cognitive radios, spectrum sharing, and deep learning.

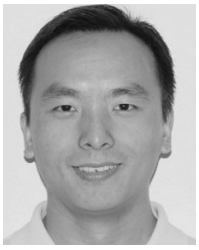

HONG-LIN ZHANG received the B.S. degree from Chongqing University, Chongqing, China, in 1999, and the M.S. and Ph.D. degrees from the South China University of Technology, Guangzhou, China, in 2008 and 2011, respectively.

Since 2012, he has been with the South China University of Technology, where he is currently an Associate Professor. From 2016 to 2017, he was a Visiting Scholar with the University of California at Los Angeles, Los Angeles. His research interests include electromagnetic field theory and applications, RF and microwave circuit techniques, and small antenna techniques. He recently focuses his research on reconfigurable RF and microwave components, digital circuit theory, and technique applied to microwave circuits.

BIN-JIE HU (M'08–SM'12) received the M.S. degree in electronic engineering from the China Research Institute of Radio Wave Propagation, Xinxiang, China, in 1991, and the Ph.D. degree in electronic engineering from the University of Electronic Science and Technology of China, Chengdu, China, in 1997.

From 1997 to 1999, he was a Postdoctoral Fellow with the South China University of Technology, Guangzhou, China. From 2001 to 2002, he was a Visiting Scholar with the Department of Electronic Engineering, City University of Hong Kong. He has been a Visiting Professor with the Universite de Nantes, France, since 2005. He is currently a Full Professor with the South China University of Technology. His current research interests include wireless communications, cognitive radios, vehicular ad hoc networks, microwave circuits, and antennas.

DESHUANG ZHAO (M'11) received the M.S. degree in electromagnetic field and microwave engineering and the Ph.D. degree in optical engineering from the University of Electronic Science and Technology of China (UESTC), Chengdu, China, in 2001 and 2005, respectively.

From March 2002 to March 2003, he was a Research Assistant with the Wireless Communications Research Centre, City University of Hong Kong. He joined UESTC, in 2005, where he is currently a Full Professor. From November 2009 to October 2010, he was a Visiting Scholar with the Department of Engineering and Aviation Science, University of Maryland Eastern Shore, USA. He has published more than 50 papers and authorized more than 20 patents. His current research interests include time reversal electromagnetics and its applications in wave field control, electromagnetic field reproduction, wireless power transfer, and green wireless communications.

YINGKUN HUANG received the B.S. degree in computer science and technology from the Southwest University, Chongqing, China, in 2011, and the M.S. degree in electric engineering from Huaqiao University, Xiamen, China, in 2015. He is currently pursuing the Ph.D. degree in electrical engineering with the Southwest Jiaotong University, Chengdu, China. His research interests include machine learning, data mining, and knowledge discovery.